

Evolution of the Pauli spin-paramagnetic effect on the upper critical fields of $K_xFe_{2-y}Se_{2-z}S_z$ single crystals

F. Wolff-Fabris,^{1,§} Hechang Lei,^{2,†,‡} J. Wosnitzer,^{1,3} and C. Petrovic^{2,‡}

¹*Hochfeld-Magnetlabor Dresden (HLD), Helmholtz-Zentrum Dresden-Rossendorf, D-01314 Dresden, Germany*

²*Condensed Matter Physics and Materials Science Department,*

Brookhaven National Laboratory, Upton, New York 11973, USA

³*Institut für Festkörperphysik, TU Dresden, D-01062, Dresden, Germany*

(Dated: November 12, 2018)

We have studied the temperature dependence of the upper critical fields, $\mu_0 H_{c2}$, of $K_xFe_{2-y}Se_{2-z}S_z$ single crystals up to 60 T. The $\mu_0 H_{c2}$ for $H \parallel ab$ and $H \parallel c$ decrease with increasing sulfur content. The detailed analysis using Werthamer-Helfand-Hohenberg (WHH) theory including the Pauli spin-paramagnetic effect shows that $\mu_0 H_{c2}$ for $H \parallel ab$ is dominated by the spin-paramagnetic effect, which diminishes with higher S content, whereas $\mu_0 H_{c2}$ for $H \parallel c$ shows a linear temperature dependence with an upturn at high fields. The latter observation can be ascribed to multiband effects that become weaker for higher S content. This results in an enhanced anisotropy of $\mu_0 H_{c2}$ for high S content due to the different trends of the spin-paramagnetic and multiband effect for $H \parallel ab$ and $H \parallel c$, respectively.

PACS numbers: 74.25.Op, 74.25.F-, 74.70.Xa

I. INTRODUCTION

Since the discovery of $LaFeAsO_{1-x}F_x$ with $T_c = 26$ K,¹ there has been considerable effort invested in understanding the properties and superconducting mechanism of iron-based superconductors.²⁻⁴ Thereby, the temperature dependence of the upper critical field, $\mu_0 H_{c2}$, attracts great interests because it provides valuable information on the coherence length, anisotropy, electronic structure, and pair-breaking mechanism. However, iron-based superconductors exhibit a rich diversity in the temperature dependence of $\mu_0 H_{c2}$. For FeAs-1111- and FeAs-122-type superconductors, such as $La(O,F)FeAs$ and $Sr(Fe,Co)_2As_2$, the upper critical fields can be described using a two-band model.^{5,6} For FeAs-111- and FeSe-11-type superconductors, such as $LiFeAs$ and $Fe(Te, Se/S)$, $\mu_0 H_{c2}$ is dominated by Pauli spin-paramagnetism.⁷⁻⁹

Studies of the upper critical field in FeSe-122-type superconductors ($A_xFe_{2-y}Se_2$, with $A = K, Rb, Cs$, or Tl) are rare because of the rather high superconducting transition temperature, T_c , and concomitantly large zero-temperature critical field. In addition, it is very challenging to handle the air-sensitive samples. Mun et al. studied $\mu_0 H_{c2}$ of $K_{0.8}Fe_{1.76}Se_2$ up to 60 T.¹⁰ They found that the upper critical field for $H \parallel c$, $\mu_0 H_{c2,c}$, increases quasi-linearly with decreasing temperature, whereas $\mu_0 H_{c2,ab}$ for $H \parallel ab$ flattens at low temperatures. The anisotropy of upper critical field, $\gamma = H_{c2,ab}/H_{c2,c}$, decreases with T and drops to about 2.5 at 18 K. A similar behavior has been observed for $Tl_{0.58}Rb_{0.42}Fe_{1.72}Se_2$.¹¹ The analysis of $\mu_0 H_{c2}$ using the Werthamer-Helfand-Hohenberg (WHH) formula including Pauli spin-paramagnetism and spin-orbit scattering indicates that spin paramagnetism plays an important role in $\mu_0 H_{c2,ab}$, whereas the enhancement of $\mu_0 H_{c2,c}$ at low temperatures is likely attributed to multiband effects.¹¹

In $K_xFe_{2-y}Se_2$, substitution of Se by sulfur suppresses T_c .¹² Preliminary measurements of $\mu_0 H_{c2}$ at low fields reveal that $\mu_0 H_{c2}$ as well decreases with S content, thereby showing temperature dependence that can be described well using the simplified WHH model without spin paramagnetism and spin-orbit scattering.¹³ However, the evolution of $\mu_0 H_{c2}$ at very high fields and low temperatures is still unclear. In this work, we report on the temperature dependence and anisotropy of upper critical fields for three single crystals with different S concentration, namely $K_{0.64}Fe_{1.44}Se_2$ (S-0), $K_{0.70(7)}Fe_{1.55(7)}Se_{1.01(2)}S_{0.99(2)}$ (S-99), and $K_{0.76(5)}Fe_{1.61(5)}Se_{0.96(4)}S_{1.04(5)}$ (S-104), accessing pulsed magnetic fields up to 60 T. We found that the spin-paramagnetic effect is rather important in $\mu_0 H_{c2,ab}$, but, at the same time, multiband effects dominate the temperature dependence of $\mu_0 H_{c2,c}$. These effects become weaker with higher S content.

II. EXPERIMENT

The single crystals of $K_xFe_{2-y}Se_{2-z}S_z$ used in this study were grown and characterized as described previously.¹² Magnetotransport experiments in pulsed magnetic fields up to 62 T were performed at the Dresden High Magnetic Field Laboratory facility, a member of the European Magnetic Field Laboratory. Exposure of the samples to ambient conditions was minimized by handling the samples in a glove box. We have used standard four-contacts technique with AC currents operating in the kHz frequency range. The electrical resistance was measured by use of a fast data-acquisition recording system and analyzed with a digital lock-in technique. The contacts were made on freshly cleaved surfaces inside a glove box using silver paint and platinum wires. The contact resistance was between 10 and 50 Ohms and the

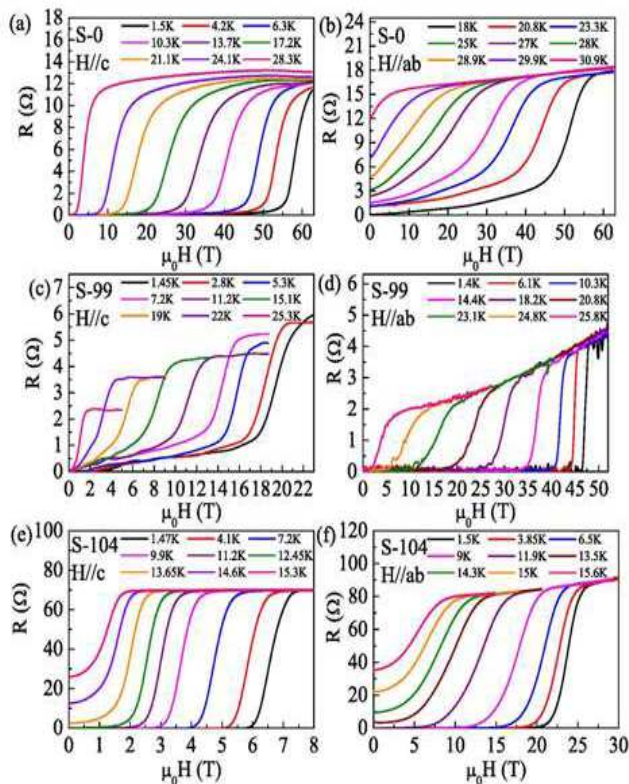


FIG. 1. (Color online) Magnetic-field dependence of the resistance, R , of sample S-0 for (a) $H \parallel c$ and (b) $H \parallel ab$, of sample S-99 for (c) $H \parallel c$ and (d) $H \parallel ab$, and of sample S-104 for (e) $H \parallel c$ and (f) $H \parallel ab$ measured at various temperatures.

excitation current was 0.3 mA which corresponds to the current density of approximately 10^3 A/m². Anisotropic measurements were conducted on the same crystal.

$K_x\text{Fe}_{2-y}\text{Se}_2$ samples are intrinsically phase separated into nanoscale magnetic insulating and Josephson-coupled superconducting regions.^{14–21} The insulating parts of the sample have several orders of magnitude higher resistance (R_i) near T_c when compared to the metallic parts (R_m).²² Therefore, near T_c and below $R(T) \approx R_m(T)$. Recent angular resolved photoemission data showed that the insulating parts of the sample do not contribute to the spectral weight in the energy range near E_F ,²³ i.e., the temperature dependence of the resistivity below T_c is dominated by the metallic parts of the sample, similar to polycrystals having dense grain boundaries. Since sulfur substitution in $K_x\text{Fe}_{2-y}\text{Se}_2$ crystals is uniform,^{12,24} S most likely substitutes both superconducting and insulating phase fractions.

III. RESULTS AND DISCUSSION

Figure 1 shows the field dependence of the resistance, R , of the samples S-0, S-99, and S-104 for $H \parallel c$ and

$H \parallel ab$ at various temperatures. Superconductivity is suppressed and the normal state recovered with increasing magnetic fields at constant temperature and the superconducting transitions in R shift to lower magnetic fields at higher temperatures. For some curves we observe a finite resistance in the superconducting state that may be caused either by experimental artifacts or by thermally activated vortex-flux motion. The experimental artifacts may include a degradation of the contacts or sample cracking during the course of the experiment. For all samples, at the same temperature, the transitions for $H \parallel ab$ occur at much higher fields when compared to those for $H \parallel c$. This shows that $\mu_0 H_{c2,ab}$ is much larger than $\mu_0 H_{c2,c}$ and that there exists a large anisotropy in the upper critical fields for all samples. On the other hand, for both field directions, the transitions rapidly shift to lower fields with increasing S content. For example, the superconducting transition at $T \sim 1.5$ K changes from about 60 to 20 T and finally reaches 7 T for the samples S-0, S-99, and S-104, respectively. This evidences that S doping significantly suppresses $\mu_0 H_{c2}$, consistent with previous results measured at low fields.^{13,25}

Figure 2 presents the temperature dependence of the resistive upper critical fields, $\mu_0 H_{c2}$, of S-0, S-99, and S-104 determined from the resistivity drops to 90% (Onset), 50% (Middle), and 10% (Zero) of the normal state resistance, R_n , for both field directions. The normal-state resistance was determined by linearly extrapolating the field-dependent resistance above the onset of the superconductivity transition. The data taken in low fields are in good agreement for S-104 crystal [Fig. 2(c)]. The S-99 crystal had $T_c \sim 26$ K, somewhat higher than crystal used in low field studies,¹³ but expected for crystals with that sulfur content.¹² For all samples, $\mu_0 H_{c2}$ obtained for $H \parallel ab$ is much larger than for $H \parallel c$, as mentioned above. The temperature dependence of $\mu_0 H_{c2,ab}$ for sample S-0 [Fig. 2(a)] is distinctively different from that of $\mu_0 H_{c2,c}$. Close to T_{c0} (zero-field transition temperature), clearly different slopes are observed in the temperature dependence of $\mu_0 H_{c2}$ for both field orientations. With decreasing temperature, the $\mu_0 H_{c2,ab}$ curves start to bend downward with a convex shape. In contrast, $\mu_0 H_{c2,c}$ exhibits almost linear temperature dependence. These results for the S-0 sample are consistent with previous measurements using a contactless rf technique.^{10,26} This suggests the absence of resistive heating in our measurements.

For the sample S-99 [Fig. 2(b)], $\mu_0 H_{c2}$ for both field directions show a similar behavior as for S-0 but the absolute values are much smaller than for the pure crystal. Moreover, T_{c0} also shifts to lower temperature. For sample S-104 [Fig. 2(c)], $\mu_0 H_{c2,ab}$ and $\mu_0 H_{c2,c}$ exhibit similar saturation trends at low temperatures with different slopes at T close to T_{c0} . When compared to the previous results measured in low fields for sample S-104, $\mu_0 H_{c2,c}$ can be well described using the simplified WHH formula, but $\mu_0 H_{c2,ab}$ is remarkably smaller than the value predicted.¹³ This implies that the temperature de-

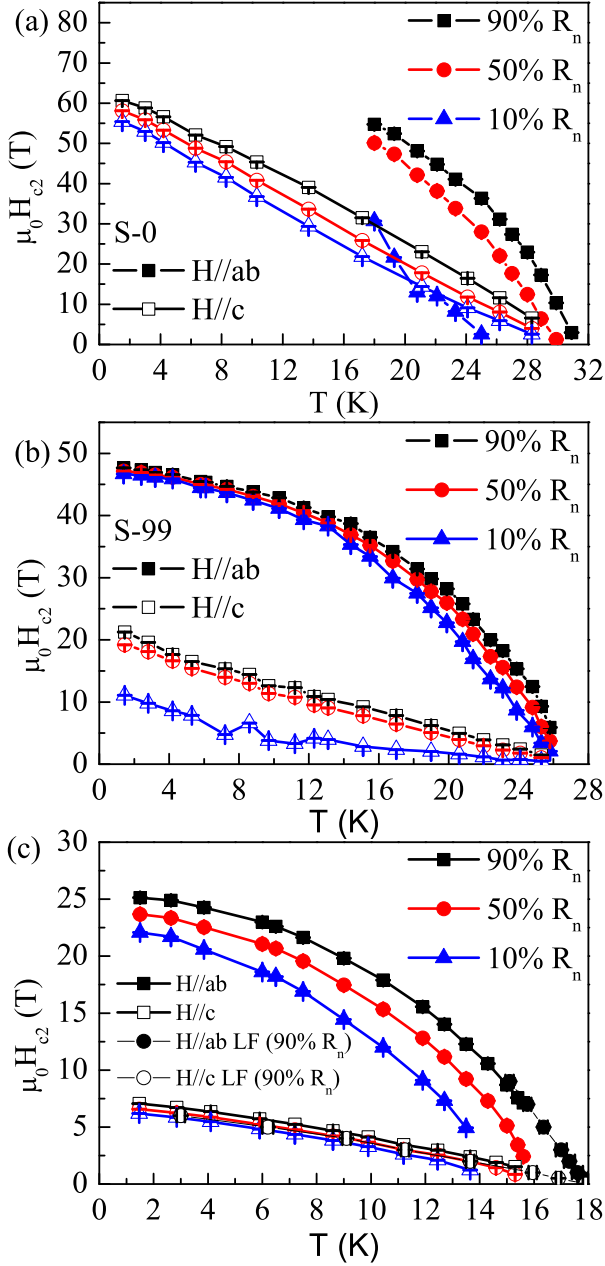


FIG. 2. (Color online) Temperature dependence of the resistive upper critical fields, $\mu_0 H_{c2}$ of the samples (a) S-0, (b) S-99, and (c) S-104 for $H \parallel ab$ (closed symbols) and $H \parallel c$ (open symbols). Figure 2 includes low field data (LF) taken on S-104 sample used in Ref. 13 for comparison

pendence of $\mu_0 H_{c2}$ is influenced by factors outside the simplified WHH model. Similarly, the nearly linear temperature dependence of $\mu_0 H_{c2,c}$ for S-0 and S-99 cannot be explained by this model.

As previous studies have shown, spin paramagnetism has a significant influence on the upper critical field of

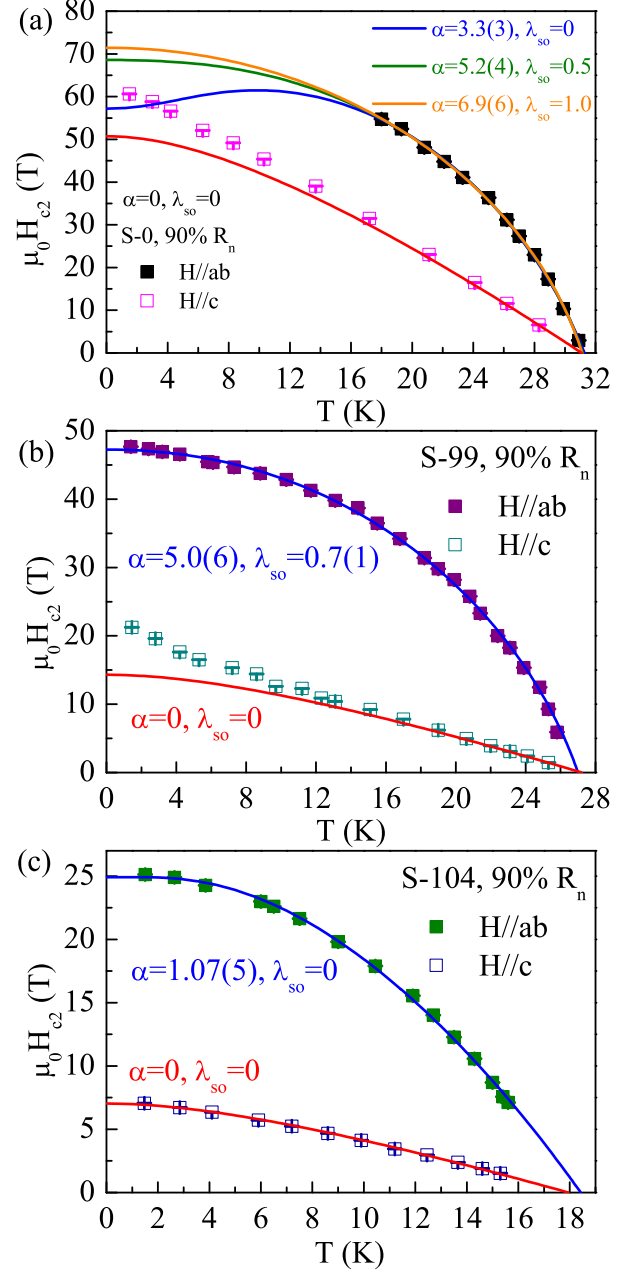


FIG. 3. (Color online) $\mu_0 H_{c2}(T)$ determined from 90% R_n (symbols) and fits using the WHH theory (solid lines) for the samples (a) S-0, (b) S-99, and (c) S-104 at $H \parallel ab$ and $H \parallel c$.

FeSe-11 and FeAs-122-type superconductors.^{8,9,27,28} We note that the Pauli paramagnetic limiting fields in simplest approximation, $\mu_0 H_P(0) = 1.86T_c$,^{29,30} are about 58.0(2) T, 50.4(2) T, and 33.8(4) T for S-0, S-99, and S-104, respectively. These values are comparable to the zero-temperature $\mu_0 H_{c2,ab}$ for these samples. This implies that the spin-paramagnetic effect needs to be considered when analyzing the temperature dependence of

$\mu_0 H_{c2}$, especially for $H \parallel ab$. Through the Maki parameter, α , and λ_{so} ³¹ the effects of Pauli spin paramagnetism and spin-orbit scattering have been included in the WHH theory for a single-band s -wave weakly coupled type-II superconductor in the dirty limit.³² $\mu_0 H_{c2}$ is given by

$$\ln \frac{1}{t} = \left(\frac{1}{2} + \frac{i\lambda_{so}}{4\gamma} \right) \psi \left(\frac{1}{2} + \frac{h + \lambda_{so}/2 + i\gamma}{2t} \right) + \left(\frac{1}{2} - \frac{i\lambda_{so}}{4\gamma} \right) \psi \left(\frac{1}{2} + \frac{h + \lambda_{so}/2 - i\gamma}{2t} \right) - \psi \left(\frac{1}{2} \right), \quad (1)$$

where $\psi(x)$ is the digamma function, $\gamma \equiv [(\alpha h)^2 - (\lambda_{so}/2)^2]^{1/2}$, and

$$h = \frac{4\mu_0 H_{c2}(T)}{\pi^2 T_c (-d\mu_0 H_{c2}(T)/dT)_{T=T_c}}. \quad (2)$$

When $\alpha > 1$, spin paramagnetism becomes essential.³¹ In Fig. 3, $\mu_0 H_{c2}$ of S-0, S-99, and S-104, determined using the 90% R_n criterion, together with the fits using formula (1) are shown. The 90% data were chosen in order to avoid the effects of flux motion and/or sample degradation. When λ_{so} is fixed to 0, $\mu_0 H_{c2,ab}$ for sample S-0 can be well described with $\alpha = 3.3(3)$ indicating strong spin paramagnetism. It should be noted that the fit is not unique and the temperature dependence of $\mu_0 H_{c2,ab}$ can as well be described with other fit values of α when λ_{so} is non-zero. This is due to the limited temperature region where data for $\mu_0 H_{c2,ab}$ are available. For different combinations of α and λ_{so} , $\mu_0 H_{c2,ab}$ varies largely at low temperatures and high fields, below our measurement range. Moreover, in order to describe $\mu_0 H_{c2}$ at low fields well, α has to increase when λ_{so} becomes larger because spin-orbit scattering tends to reduce the effect of spin paramagnetism.³² Accordingly, $\alpha = 3.3(3)$ is a lower limit. On the other hand, the WHH model with $\alpha = 0$ and $\lambda_{so} = 0$ does not describe the curve well. Thus, even though α and λ_{so} are not uniquely determined by our data, the large $\alpha = 3.3(3)$ strongly indicates that spin paramagnetism plays an important role in suppressing superconductivity for $H \parallel ab$. This sample might be worth to investigate in even higher magnetic fields by using a 100 T coil in order to explore the evolution of paramagnetic effects for $H \parallel ab$.

For $H \parallel c$, $\mu_0 H_{c2,c}$ at low temperatures is enhanced when compared to the WHH model. Such an enhancement cannot be explained by $\alpha > 0$ or $\lambda_{so} > 0$. Indeed, it suggests that multiband effect become important when the magnetic field is oriented along the c direction. A similar behavior has been observed in $\text{Tl}_{0.58}\text{Rb}_{0.42}\text{Fe}_{1.72}\text{Se}_2$.¹¹

Increasing the S content to 0.99, $\mu_0 H_{c2,ab}$ is suppressed to below 50 T in the whole temperature range [Fig. 3(b)]. Without considering spin-orbital scattering, the WHH formula cannot describe $\mu_0 H_{c2,ab}$ well even when including spin paramagnetism. When the spin-orbit scattering term is included, the fit quality improves significantly and the obtained parameters are $\alpha = 5.0(6)$ and $\lambda_{so} = 0.7(1)$.

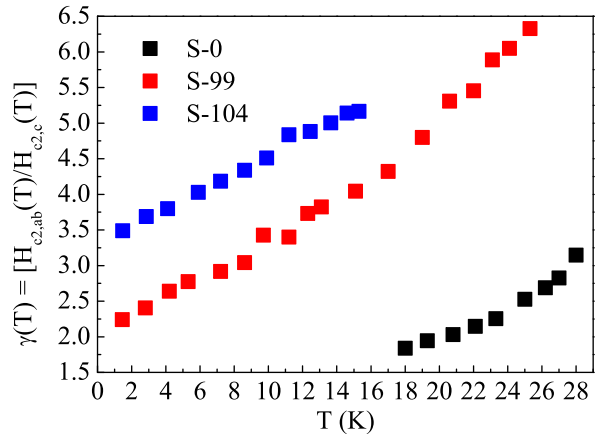


FIG. 4. (Color online) Temperature dependence of the anisotropy, $\gamma = H_{c2,ab}/H_{c2,c}$ using the 90% R_n criterion for the samples S-0, S-99, and S-104.

Assuming $\lambda_{so} = 0.7$ for the sample S-0, α in sample S-0 will be larger than in sample S-99. On the other hand, $\mu_0 H_{c2,c}$ shows a linear temperature dependence down to about 8 K, below which an upturn appears. As for the pure sample, this upturn cannot be described by use of the simplified WHH model. This shows that multiband effects are still important in sample S-99 for $H \parallel c$.

For the single-band clean limit, the Maki parameters for $H \parallel ab$ and $H \parallel c$ should be related by the ratio of the Fermi velocity v_{ab} in the ab plane to v_c along c . The cylinder-like Fermi surface in iron-based superconductors results in $v_{ab} \gg v_c$. Therefore, this ratio is larger than 1 and the α for $H \parallel ab$ is expected to be larger than for $H \parallel c$,³³ i.e., spin paramagnetism is stronger for $H \parallel ab$ than for $H \parallel c$. The open electronic orbits along c reduce the orbital-limited upper critical field considerably.¹¹

With further S substitution [sample S-104, Fig. 3(c)], the WHH model without spin-orbit scattering can describe the temperature dependence of $\mu_0 H_{c2,ab}$ well with $\alpha = 1.07(5)$. This is somewhat larger than 1, suggesting that spin paramagnetism is still essential. But, the absolute value is much smaller than for the samples S-0 and S-99. Obviously, α decreases with increasing S content, i.e., spin paramagnetism becomes less important. The $\mu_0 H_{c2,c}$ can be well described by using the WHH formula without including spin paramagnetism or spin-orbit scattering. The slope $-d(\mu_0 H_{c2,c})/dT$ near T_{c0} is 0.565(5) T/K, which is very close to the previous results measured at low fields.¹³ Our results show that the multiband as well as possible spin-paramagnetic effects are largely suppressed in S-104 for $H \parallel c$.

The anisotropy of the upper critical field, $\gamma = H_{c2,ab}/H_{c2,c}$, supplies further information on the effect of S substitution on the evolution of $\mu_0 H_{c2}$. As shown in Fig. 4, γ exhibits a similar trend in the temperature-dependence for all three samples: the anisotropy de-

creases considerably with temperature. For sample S-0, γ is ~ 3.1 at 28 K and decreases to ~ 1.8 at 18 K, a somewhat smaller value than reported in literature.¹⁰ For sample S-99, γ is about 6.3 at 25 K and decreases gradually to ~ 2.2 at 1.5 K. Finally, for sample S-104, γ lies between ~ 5.2 at 15 K and ~ 3.5 at 1.5 K. This trend has been observed in all iron-based superconductors.^{33,34}

The origin of the small anisotropy of the upper critical fields could be caused by a three-dimensional electronic structure, spin paramagnetism, or multiband effects.³⁴ The notable outcome of our study is that the anisotropy increases with S content, consistent with previous results measured in the Ginzburg-Landau region where it was speculated that this might be due to a smaller warping of the two-dimensional (2D) Fermi surface (FS) with increasing S content.¹³ The increase of the anisotropy with S substitution is understandable since orbital pair breaking is more effective near T_{c0} ,³⁴ and a more 2D FS should lead to a larger γ . However, this work shows that other factors can as well result in an enhanced anisotropy of $\mu_0 H_{c2}$ in the high-field low-temperature region. First, spin paramagnetism which usually decreases the anisotropy of the upper critical field at high fields becomes weaker with increasing S content, thus the suppression of $\mu_0 H_{c2,ab}$ is reduced. Second, multiband effects also become weaker at higher S content, and the slight upturn of $\mu_0 H_{c2,c}$ at high fields changes to a saturation behavior described by the WHH model. These two opposite trends contribute to a larger γ . Since α is proportional to the effective mass in the clean limit,³⁵ the smaller α with increasing S content can partially be related to a decrease of the effective mass.^{33,36} The decrease in α is in agreement with suppression of spin susceptibility and spin excitations in $K_x\text{Fe}_{2-y}\text{Se}_{1-z}\text{S}_z$.³⁷ In addition,

sulfur substitution might also change the electronic structure leading to reduced multiband effects. Further theoretical work is necessary to clarify this.

IV. CONCLUSION

In summary, we have investigated the upper critical fields of $K_x\text{Fe}_{2-y}\text{Se}_{1-z}\text{S}_z$ single crystals up to 60 T. The $\mu_0 H_{c2}$ for both $H \parallel ab$ and $H \parallel c$ decreases with increasing S content. For $H \parallel ab$, the $\mu_0 H_{c2,ab}$ follows the WHH model including strong spin paramagnetism. The $\mu_0 H_{c2,c}$ for low S content shows a behavior that suggests multiband effects and the single-band orbitally limited field gradually becomes dominant at high sulfur content. The anisotropy of $\mu_0 H_{c2}$ is enhanced with increasing S content which can be explained by weakened spin paramagnetism and reduced multiband effects for $H \parallel ab$ and $H \parallel c$, respectively.

V. ACKNOWLEDGEMENTS

Work at Brookhaven is supported by the Center for Emergent Superconductivity, an Energy Frontier Research Center funded by the U.S. DOE, Office for Basic Energy Science (HL and CP). Part of this work was supported by EuroMagNET II (EU Contract No. 228043). CP acknowledges support by the Alexander von Humboldt Foundation.

§Current Address: European XFEL GmbH, Notkestrasse 85, 22607, Hamburg, Germany.

† Current Address: Frontier Research Center and Materials and Structures Laboratory, Tokyo Institute of Technology, 4259 Nagatsuta, Midori, Yokohama 226-8503, Japan

‡ hlei@lucid.msl.titech.ac.jp and petrovic@bnl.gov

-
- ¹ Y. Kamihara, T. Watanabe, M. Hirano, and H. Hosono, *J. Am. Chem. Soc.* **130**, 3296 (2008).
- ² G. R. Stewart, *Rev. Mod. Phys.* **83**, 1589 (2011).
- ³ E. Dagotto, *Rev. Mod. Phys.* **85**, 849 (2013).
- ⁴ Jianping Hu and Ningning Hao, *Phys. Rev. X* **2**, 021009 (2012).
- ⁵ F. Hunte, J. Jaroszynski, A. Gurevich, D. C. Larbalestier, R. Jin, A. S. Sefat, M. A. McGuire, B. C. Sales, D. K. Christen, and D. Mandrus, *Nature* **453**, 903 (2008).
- ⁶ S. A. Baily, Y. Kohama, H. Hiramatsu, B. Maiorov, F. F. Balakirev, M. Hirano, and H. Hosono, *Phys. Rev. Lett.* **102**, 117004 (2009).
- ⁷ S. Khim, B. Lee, J. W. Kim, E. S. Choi, G. R. Stewart, and K. H. Kim, *Phys. Rev. B* **84**, 104502 (2011).
- ⁸ H. C. Lei, R. W. Hu, E. S. Choi, J. B. Warren, and C. Petrovic, *Phys. Rev. B* **81**, 094518 (2010).
- ⁹ H. C. Lei, R. W. Hu, E. S. Choi, J. B. Warren, and C. Petrovic, *Phys. Rev. B* **81**, 184522 (2010).
- ¹⁰ E. D. Mun, M. M. Altarawneh, C. H. Mielke, V. S. Zapf, R. Hu, S. L. Bud'ko, and P. C. Canfield, *Phys. Rev. B* **83**, 100514(R) (2011).
- ¹¹ L. Jiao, Y. Kohama, J. L. Zhang, H. D. Wang, B. Maiorov, F. F. Balakirev, Y. Chen, L. N. Wang, T. Shang, M. H. Fang, and H. Q. Yuan, *Phys. Rev. B* **85**, 064513 (2012).
- ¹² H. C. Lei, M. Abeykoon, E. S. Bozin, K. F. Wang, J. B. Warren, and C. Petrovic, *Phys. Rev. Lett.* **107**, 137002 (2011).
- ¹³ H. C. Lei and C. Petrovic, *Europhys. Lett.* **95**, 57006 (2011).
- ¹⁴ D. H. Ryan, W. N. Rowan-Weetaluktuk, J. M. Cadogan, R. Hu, W. E. Straszheim, S. L. Budko, and P. C. Canfield, *Phys. Rev. B* **83**, 104526 (2011).
- ¹⁵ Z. Wang, Y. J. Song, H. L. Shi, Z. W. Wang, Z. Chen, H. F. Tian, G. F. Chen, J. G. Guo, H. X. Yang, and J. Q. Li, *Phys. Rev. B* **83**, 140505 (2011).
- ¹⁶ Y. Liu, Q. Xing, K. W. Dennis, R. W. McCallum, and T. A. Lograsso, *Phys. Rev. B* **86**, 144507 (2012).
- ¹⁷ A. Ricci, N. Poccia, B. Joeseph, G. Arrighetti, L. Barba, J. Plaiser, G. Campi, Y. Mizuguchi, H. Takeya, Y. Takano, N. L. Saini, and A. Bianconi, *Supercond. Sci. Technol.* **24**, 082002 (2011).
- ¹⁸ Wei Li, H. Ding, P. Deng, K. Chang, C. Song, Ke He, L.

- Wang, X. Ma, J. P. Hu, X. Chen, and Q.K. Xue, *Nature Physics* **8**, 126 (2012).
- ¹⁹ R. H. Yuan, T. Dong, Y. J. Song, P. Zheng, G. F. Chen, J. P. Hu, J. Q. Li, and N. L. Wang, *Sci. Rep.* **2**, 221 (2012).
- ²⁰ D. Louca, K. Park, B. Li, J. Neufeind, and J. Yan, *Sci. Rep.* **3**, 2047 (2013).
- ²¹ N. Lazarevic, M. Abeykoon, P. W. Stephens, Hechang Lei, E. S. Bozin, C. Petrovic, and Z. V. Popovic, *Phys. Rev. B* **86**, 054503 (2012).
- ²² D. P. Shoemaker, D. Y. Chung, H. Claus, M. C. Francisco, S. Avci, A. Llobet, and M. G. Kanatzidis, *Phys. Rev. B* **86**, 184511 (2012).
- ²³ M. Yi, D. H. Lu, R. Yu, S. C. Riggs, J.-H. Chu, B. Lv, Z. K. Liu, M. Lu, Y.-T. Cui, M. Hashimoto, S.-K. Mo, Z. Hussain, C. W. Chu, I. R. Fisher, Q. Si, and Z.-X. Shen, *Phys. Rev. Lett.* **110**, 067003 (2013).
- ²⁴ Hechang Lei and C. Petrovic, *Phys. Rev. B* **84**, 052507 (2011).
- ²⁵ J. J. Ying, X. F. Wang, X. G. Luo, A. F. Wang, M. Zhang, Y. J. Yan, Z. J. Xiang, R. H. Liu, P. Cheng, G. J. Ye, and X. H. Chen, *Phys. Rev. B* **83**, 212502 (2011).
- ²⁶ V. A. Gasparov, A. Audouard, L. Drigo, A. I. Rodigin, C. T. Lin, W. P. Liu, M. Zhang, A. F. Wang, X. H. Chen, H. S. Jeevan, J. Maiwald and P. Gegenwart, *Phys. Rev. B* **87**, 094508 (2013).
- ²⁷ V. A. Gasparov, F. Wolff-Fabris, D. L. Sun, C. T. Lin and J. Wosnitza, *JETP Lett.* **93**, 26 (2011).
- ²⁸ V. A. Gasparov, L. Drigo, A. Audouard, D. L. Sun, C. T. Lin, S. L. Bud'ko, P. C. Canfield, F. Wolff-Fabris and J. Wosnitza, *JETP Lett.* **93**, 667 (2001).
- ²⁹ B. S. Chandrasekhar, *Appl. Phys. Lett.* **1**, 7 (1962).
- ³⁰ A. M. Clogston, *Phys. Rev. Lett.* **9**, 266 (1962).
- ³¹ K. Maki, *Phys. Rev.* **148**, 362 (1966).
- ³² N. R. Werthamer, E. Helfand, and P. C. Hohenberg, *Phys. Rev.* **147**, 295 (1966).
- ³³ H. C. Lei, K. F. Wang, R. Hu, H. J. Ryu, M. Abeykoon, E. S. Bozin, and C. Petrovic, *Sci. Technol. Adv. Mater.* **13**, 054305 (2012).
- ³⁴ J.-L. Zhang, L. Jiao, Y. Chen, and H.-Q. Yuan, *Front. Phys.* **6**, 463 (2011).
- ³⁵ A. Gurevich, *Rep. Prog. Phys.* **74**, 124501 (2011).
- ³⁶ K. F. Wang, H. C. Lei, and C. Petrovic, *Phys. Rev. B* **84**, 054526 (2011).
- ³⁷ D. A. Torchetti, T. Imai, H. C. Lei and C. Petrovic, *Phys. Rev. B* **85**, 144516 (2012).